National Research Council Canada
Conseil national de recherches Canada

Division of Electrical Engineering
Division de génie électrique

ERB-990

Facility for Measurements of the Electromagnetic Backscattering Matrix Elements of a Single Body

L.E. Allan, Y.M.M. Antar, and A. Hendry

May 1986

Canada

NRCC No. 26138

86-06456/

Copyright 1986 by
National Research Council of Canada

Permission is granted to quote short excerpts and to reproduce figures and tables from this report, provided that the source of such material is fully acknowledged.

Copyright 1986 par
Conseil national de recherches du Canada

Il est permis de citer de courts extraits et de reproduire des figures ou tableaux du présent rapport, à condition d'en identifier clairement la source.

Additional copies are available free of charge from:

Editorial Office, Room 301
Division of Electrical Engineering
National Research Council of Canada
Ottawa, Ontario, Canada
K1A 0R8

Des exemplaires supplémentaires gratuits peuvent être obtenus à l'adresse suivante:

Bureau des publications, Pièce 301
Division de génie électrique
Conseil national de recherches du Canada
Ottawa (Ontario) Canada
K1A 0R8

FACILITY FOR MEASUREMENTS OF THE ELECTROMAGNETIC BACKSCATTERING MATRIX ELEMENTS OF A SINGLE BODY

L.E. Allan, Y.M.M. Antar, and A. Hendry

ERB-990

NRCC No. 26138

May 1986

TABLE OF CONTENTS

		Page
ABSTRACT/RÉSUMÉ		v
1	INTRODUCTION	1
2	RÉSUMÉ OF THEORY	3
3	MICROWAVE APPARATUS	6
4	ISOLATION, MATCHING, AND LEAKAGE SUPPRESSION MEASURES	17
5	NULLING PROCEDURE	19
6	RECEIVING SYSTEM	19
7	DATA ACQUISITION SYSTEM	23
8	CALIBRATION	24
9	PERFORMANCE AND TECHNICAL SPECIFICATIONS	26
10	EXPERIMENTAL PROCEDURE	29
11	DATA RECORDING FORMAT AND INTERPRETATION	30
12	ERROR CORRECTION AND NORMALIZATION	30
13	SAMPLE OF RESULTS	31
ACKNOWLEDGEMENT		32
REFERENCES		32

LIST OF FIGURES

1	Coordinate system and scattering geometry	4
2	Rotation of particle with respect to coordinate axes	4
3	9.6 GHz microwave apparatus	6
4	Basic features of scattering measurement set-up	7
5	9.6 GHz horn and turnstile assembly	8
6	Complete block diagram of scattering system	10
7	X-band horn antenna amplitude patterns: (a) Port 1, elevation plane, (b) Port 2, elevation plane, (c) Port 1, azimuth plane, (d) Port 2, azimuth plane	11
8	X-band horn antenna polarization patterns, showing axial ratios at various points in the main beam	15
9	Amplitude and phase tuner assembly	17
10	Isolation and VSWR of turnstile and horn	18
11	Nulling procedure	20
12	Receiving system	21
13	Receiver transfer characteristics	22
14	Phase error matrix	22
15	Video processor and data recording system	23
16	Phase calibration procedure	25
17	Amplitude calibration procedure	27
18	Determination of K(R) for X-band system	28
19	Sample of results for a dielectric rod	31

ABSTRACT

A two-channel laboratory facility for measuring the circularly polarized backscattering matrix elements of single dielectric bodies is described. The system consists of a circularly polarized horn antenna fed by a turnstile junction, a highly stable c-w signal source, and a two-channel receiver. Either sense of circular polarization may be radiated. Simultaneous reception of both RHC and LHC components of the backscattered wave and measurement of their relative phase are provided for. Two sets of equipment have been built; these operate at 2.862 GHz and at 9.600 GHz, respectively. The report describes the design and performance of these equipments and includes a sample of the results obtained.

RÉSUMÉ

Un montage de laboratoire à deux voies de mesure des éléments de la matrice de rétrodiffusion en polarisation circulaire de corps diélectriques est décrit. Il se compose d'un cornet à polarisation circulaire alimenté par une jonction tourniquet, d'une source de signal à ondes entretenues extrêmement stable et d'un récepteur deux voies. La polarisation circulaire peut se faire dans les deux sens. Il est possible de recevoir simultanément les composantes PCD et PCG de l'onde rétrodiffusée et de mesurer leur déphasage relatif. Deux montages ont été réalisés; un fonctionne sur 2,862 GHz, l'autre sur 9,600 GHz. Le présent document décrit la conception et précise la performance de ces montages et fournit un échantillon des résultats obtenus.

FACILITY FOR MEASUREMENTS OF THE ELECTROMAGNETIC BACKSCATTERING MATRIX ELEMENTS OF A SINGLE BODY

L.E. Allan, Y.M.M. Antar, and A. Hendry

1. INTRODUCTION

As part of a program of radar meteorology in which scattering and wave propagation in precipitation media are measured by a dual-channel circularly polarized radar system, a facility has been established for measuring the backscattering matrix, at circular polarization, of single dielectric objects. One of the purposes of this work is to provide results on bodies of known geometry and dielectric properties which would be useful for the interpretation and confirmation of the radar results obtained from tropospheric data. However, the data obtained are of wider interest, and the results are scientifically interesting in their own right. This report deals with the apparatus used in the experiment. Also included is a summary of the theoretical relationship involved in the backscattering matrix.

Although considerable progress has been made in recent years in computational techniques, it is necessary to have experimental data to augment theoretical calculations, because the latter remain just that until confirmed by measurements. Furthermore, computational techniques are generally limited to the treatment of shapes which can be readily described analytically. For irregular or complex objects, experimental measurement techniques are essential.

In the past, scattering matrix measurements have often been limited to amplitudes only. The complete description of the scattering characteristics of an object requires knowledge of the phase as well. The apparatus described in this report provides for determination of the amplitudes and relative phase of the scattering matrix elements, but not the absolute phase. However, the latter quantity is usually not of interest.

Since the radar system used for atmospheric studies employs circular polarizations, similar polarization base vectors, i.e., RHC and LHC, were adopted for the scattering matrix apparatus. Matrix elements for other polarizations are readily available from simple transformations. The use of circular polarizations has some natural advantages: (i) The differential phase shift in the scattering process is larger for circular than for linear polarizations, and thus it is easier to measure; (ii) the scattering matrix may be expressed in a very simple form for bodies of revolution.

No matter what polarization is chosen for the system, it is essential that there be a high degree of polarization purity in the illuminating wave and that the illumination intensity be as uniform as possible in both amplitude and phase over the "active area," within which the object whose scattering matrix is to be determined is positioned. For the apparatus described here, the illumination source consists of a dual mode conical horn antenna, fed from a turnstile junction, the latter being adjusted to produce either RHC or LHC, depending upon the waveguide port chosen for transmission. This combination is capable of generating very pure circular polarization over a wide beamwidth. It is also capable of providing high isolation between ports. The latter characteristic is extremely important, since the ability of the system to accurately measure the very small cross-polarized components of the backscatter from nearly symmetric targets would be thwarted unless the cross-coupling between ports is very small. However, the bandwidth over which the combination of high isolation and polarization purity is achieved is quite narrow for this type of illuminator.

In order to maintain a compact set-up, it is necessary to position the object whose scattering matrix is being measured close to the illuminating antenna. If a pulsed system were used, a very short pulse would be required. For example, a minimum range of 1.5 m dictates a maximum pulse length of 10 ns to achieve temporal separation of the echo and transmitted pulse. Unfortunately, the bandwidth required for such a narrow pulse exceeds that over which good isolation and polarization purity exists in the illuminator. For this and other reasons, the system uses continuous-wave (c-w) illumination.

The use of c-w, while simplifying some problems, introduces others. Since the transmitted and reflected waves exist simultaneously, it is necessary to cancel or null out any portion of the transmitted wave which enters the receivers by paths other than by direct backscattering from the target object. Such other paths exist within the microwave transmission structure, and a succeeding section of the report will describe in detail the measures taken to achieve the required nulling. Other ways in which an unwanted portion of the transmitted wave may enter the receiver include internal reflections in the microwave structure, direct or multiple reflections of the transmitted wave by material objects in the vicinity of the radiating illuminator, and spurious reflecting objects, such as insects or precipitation particles which may enter the beam.

To reduce unwanted reflections to acceptable levels, the apparatus is operated out-of-doors at an unobstructed site, with the incident beam directed vertically upwards. This virtually eliminates unwanted reflections from structures, but imposes the limitations that observations can only be made under clear and calm atmospheric conditions, and precautions have to be taken that birds or insects do not upset the results.

The objects under test must be positioned vertically above the illuminating antenna and provision made for rotation of the objects about a fixed axis. Ideally, the supports for the objects should be "invisible," i.e., the backscattering from the supports should be much less than the weakest component to be measured. These requirements are discussed more fully below.

The methods used for nulling out unwanted signals depend for their success on the use of a highly stable signal source and on thermal stability of the equipment. For the latter requirement, the entire microwave apparatus, except for the radiating horn, is contained in an insulated enclosure within which the ambient temperature is closely controlled.

To reduce the amount of equipment used for this experiment, the receivers and data acquisition apparatus which form part of the NRC precipitation radar are used. Such sharing of apparatus works well, because the clear conditions under which the scattering experiment is done are rarely of interest from a precipitation-radar point of view.

2. RÉSUMÉ OF THEORY

A theoretical discussion of backscattering in terms of circular polarization base vectors from targets possessing a symmetry plane is contained in ref. 1. This section summarizes the theory necessary for treating the backscatter from single dielectric objects.

The geometry of the target relative to the illuminating antenna is shown in Fig. 1. The received fields at the antenna in terms of the fields incident on the target are given by

$$[1] \qquad \begin{bmatrix} E_x \\ E_y \end{bmatrix}^r = \frac{e^{-jkR}}{R} \begin{bmatrix} S_{xx} & 0 \\ 0 & S_{yy} \end{bmatrix} \begin{bmatrix} E_x \\ E_y \end{bmatrix}^i$$

where E_x^i, E_y^i are the incident fields at the scatterer and E_x^r, E_y^r are the received fields at the horn antenna. For a symmetrical target with a symmetry axis in the XOZ plane (as shown in Fig. 2) the off-diagonal terms vanish. For circular polarization base vectors (E_+, E_-):

$$[2] \qquad \begin{bmatrix} E_+ \\ E_- \end{bmatrix}^r = \frac{e^{-jkR}}{R} [S^c] \begin{bmatrix} E_+ \\ E_- \end{bmatrix}^i$$

$$= \frac{e^{-jkR}}{R} \begin{bmatrix} S_{xx} - S_{yy} & S_{xx} + S_{yy} \\ S_{xx} + S_{yy} & S_{xx} - S_{yy} \end{bmatrix} \begin{bmatrix} E_+ \\ E_- \end{bmatrix}^i$$

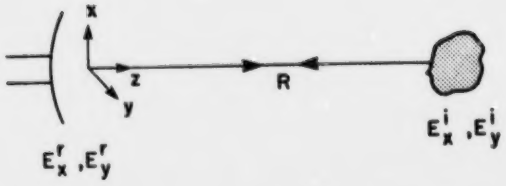

Figure 1. Coordinate system and scattering geometry

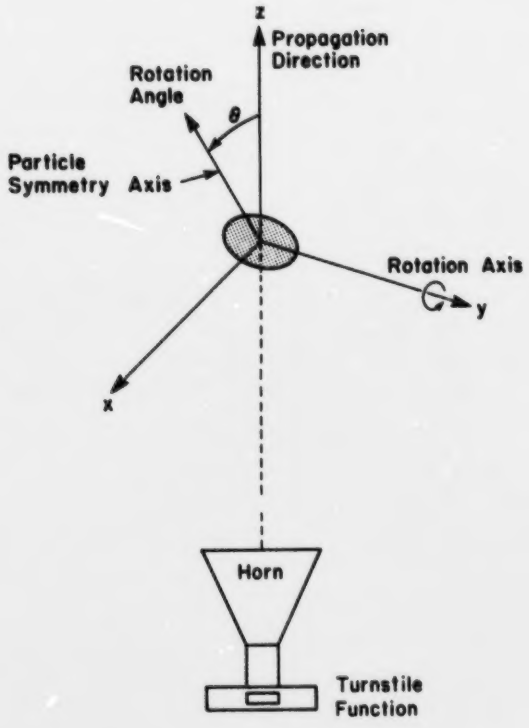

Figure 2 Rotation of particle with respect to coordinate axes

where the + and - subscripts denote RHC and LHC polarizations, respectively. S^C is the scattering matrix for circular base vectors.

For RHC incidence, $\begin{bmatrix} E_+ \\ E_- \end{bmatrix} i = \begin{bmatrix} 1 \\ 0 \end{bmatrix}$, or LHC incidence, $\begin{bmatrix} E_+ \\ E_- \end{bmatrix} i = \begin{bmatrix} 0 \\ 1 \end{bmatrix}$, $(S_{xx} - S_{yy})$ is the same sense return, and $(S_{xx} + S_{yy})$ is the orthogonal or main return.

Define σ and η as follows:

[3] $$\sigma = \pi \left| S_{xx} + S_{yy} \right|^2$$

[4] $$\eta = \nu e^{i\delta} = \frac{S_{xx} - S_{yy}}{S_{xx} + S_{yy}}$$

where σ is the circular polarization radar cross section, ν is the amplitude relationship between the two returns, and δ is the phase relationship between the two returns.

S^C may be written as

$$[5] \qquad S^c = \frac{1}{2}\left(\frac{\sigma}{\pi}\right)^{1/2} e^{i\phi} \begin{bmatrix} \nu e^{i\delta} & 1 \\ 1 & \nu e^{i\delta} \end{bmatrix}$$

where

$$\phi = \text{Arg}\ (S_{xx} - S_{yy})$$

is the absolute phase.

Thus measurement of σ, ν, and δ provides a complete determination of S^c apart from the phase factor ϕ.

The relationships of these factors to the linear polarization base vectors are given by:

$$[6] \qquad S_{xx} = \frac{1}{2}\left(\frac{\sigma}{\pi}\right)^{1/2} e^{i\phi}\ (1 + \eta)$$

$$[7] \qquad S_{yy} = \frac{1}{2}\left(\frac{\sigma}{\pi}\right)^{1/2} e^{i\phi}\ (1 - \eta)$$

$$[8] \qquad \sigma_x = 4\pi\left|S_{xx}\right|^2 = \sigma(1 + \nu^2 + 2\nu \cos\ \delta)$$

$$[9] \qquad \sigma_y = 4\pi\left|S_{yy}\right|^2 = \sigma(1 + \nu^2 - 2\nu \cos\ \delta)$$

$$[10] \qquad \tan\ \Delta = \left[2\nu/(1 - \nu^2)\right] \sin\ \delta$$

where

$$\Delta = \text{Arg}\ (S_{xx}\ S_{yy}^*)$$

is the backscatter differential phase shift at linear polarization.

The received signals R_1 and R_2, for transmission at either port (RHC or LHC), are given by

$$[11] \qquad \begin{bmatrix} R_1 \\ R_2 \end{bmatrix}_{\pm} \cong K(R)\sigma^{1/2} \begin{bmatrix} \eta + 2\varepsilon_{\pm} \\ 1 \end{bmatrix}$$

where K(R), an empirical function of the range R, is determined using backscattering data from small metallic spheres at various values of R. $\varepsilon_{\pm}$ is an error term also determined from Equation [11] using small metallic spheres, for which ν and therefore η is very close to zero.

There are four output voltages from the system; these are proportional to the following four quantities:

$(R_1 R_1^*)^{1/2}$ $\cos (\text{Arg } R_1 R_2^*)$
$(R_2 R_2^*)^{1/2}$ $\sin (\text{Arg } R_1 R_2^*)$,

The cos and sin functions provide in-phase and quadrature components of the relative phase of R_1 and R_2. Measurement of an object at both RHC and LHC provides **two independent sets of measurements.**

3. MICROWAVE APPARATUS

Two functionally identical sets of apparatus have been built. The first of these operates in the 10 cm wavelength region, with a transmitter

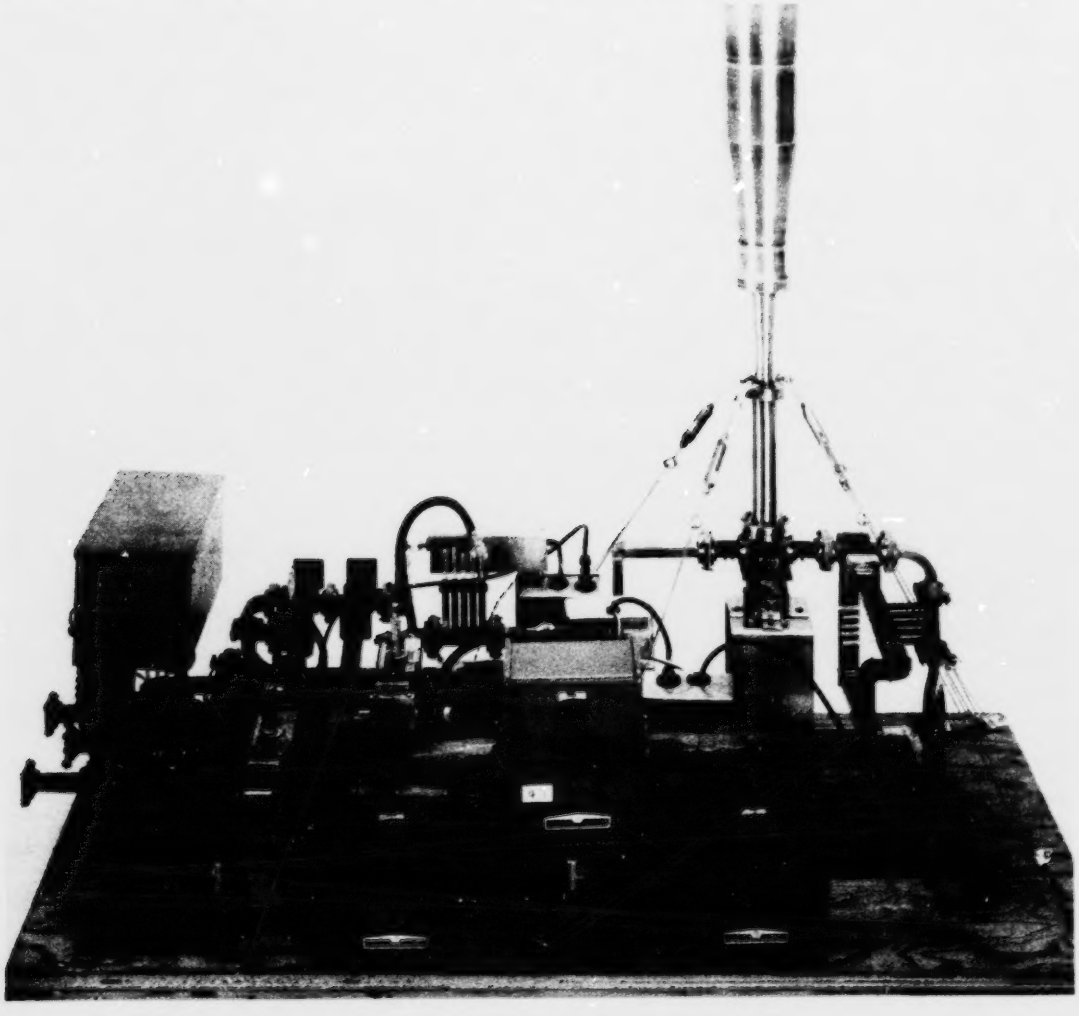

Figure 3. 9.6 GHz microwave apparatus

frequency of 2.8618 GHz, while the second (see Fig. 3) operates at 9.6000 GHz. The basic features of the systems are shown in Fig. 4. The output signal from a phase-locked oscillator is delivered via the switch S to either Port 1 or Port 2 of a turnstile junction, the latter being connected to a horn antenna whose beam illuminates the object to be measured. The turnstile junction is so adjusted that inputs to Port 1 and Port 2 generate, respectively, right-hand and left-hand circularly polarized waves in the circular waveguide portion of the junction. The choice of radiated polarization is thus governed by the position of switch S. The antenna is a dual mode horn of the type described by Potter (2) and is characterized by excellent polarization purity over a narrow band. Figure 5 shows the 9.6 GHz horn and turnstile assembly.

The object under test is therefore illuminated by a circularly polarized wave. The backscattered wave from the object will, in general, be elliptically polarized; on reception it is resolved by the horn and turnstile into its RHC and LHC polarized components, which then emerge from the turnstile via Ports 1 and 2, respectively. These echo components are converted to signals at a frequency of 30 MHz by the mixer-preamplifier units as shown, and then conveyed via coaxial cables to the equipment room containing the radar receivers, where signal processing takes place.

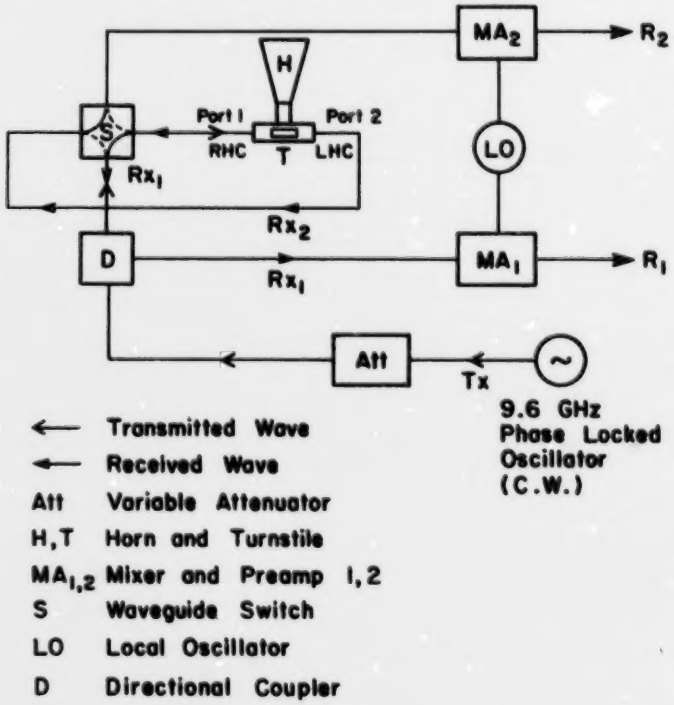

Figure 4. Basic features of scattering measurement set-up

Figure 5. 9.6 GHz horn and turnstile assembly

Figure 6 is a more complete block diagram of the system showing most of the functionally important elements. Provision is made, via switches, tuners, attenuators, and directional couplers for calibration, nulling of unwanted leakage and reflections, and for adjusting the operating power range in circumstances where either the echo power is out of the linear range of the receivers or the dynamic range requirement cannot be met at a single power setting. These aspects will be discussed in later sections of this report.

The output signal from the source oscillator (+14.2 dBm at X-band, +18.8 dBm at S-band) is amplified to a level of 27 dBm (at X-band). A sample of this signal is used for continuous monitoring of the power and frequency of the source. The source oscillators are crystal controlled, with overall stabilities of ±0.0005% at X-band, ±0.002% at S-band. The signal paths during measurements are as indicated in Fig. 6.

The design and adjustment of the turnstile junction follows standard procedure as described by Ragan (3). With shorting plungers on two opposing rectangular waveguide arms, circular polarizations are generated in the two circular mode ports when the distances to the plungers differ by $\lambda/4$ and the positions of the plungers are so adjusted as to produce a $\pi/2$ phase difference between linearly polarized components in the circular waveguide.

The S-band and X-band horn antennas are scaled versions, i.e., their dimensions in terms of wavelength are identical, and therefore such electrical characteristics as beamwidth and gain are close to identical. The characteristics of the X-band horn are: beamwidth 19.6°, gain approximately 21 dBi, and axial ratio 0.974 to 0.996. Figures 7 and 8 show sample amplitude and polarization patterns. The horn length and aperture are 53.3 and 11.7 cm, respectively. The antenna is characterized by low sidelobe levels and good circular polarization purity.

Two separate types of tuners are used in the waveguide system for nulling and matching purposes. The tuners designated T_1 and T_2 in Fig. 6 comprise, in series, a five-probe low leakage tuner, a slide-screw tuner, and a matched termination. This assembly, which is connected to one arm of a wave-guide ferrite circulator (see Fig. 9), allows for continuous variation of the amplitude and phase of the signal emerging from the third port of the circulator. The tuners designated T, T_L, and T_R are five-probe tuners designed for low leakage.

The directional couplers designated D in Fig. 6 are standard 20 dB crossguide couplers. D_2 is a multi-hole high directivity 3-dB coupler, its

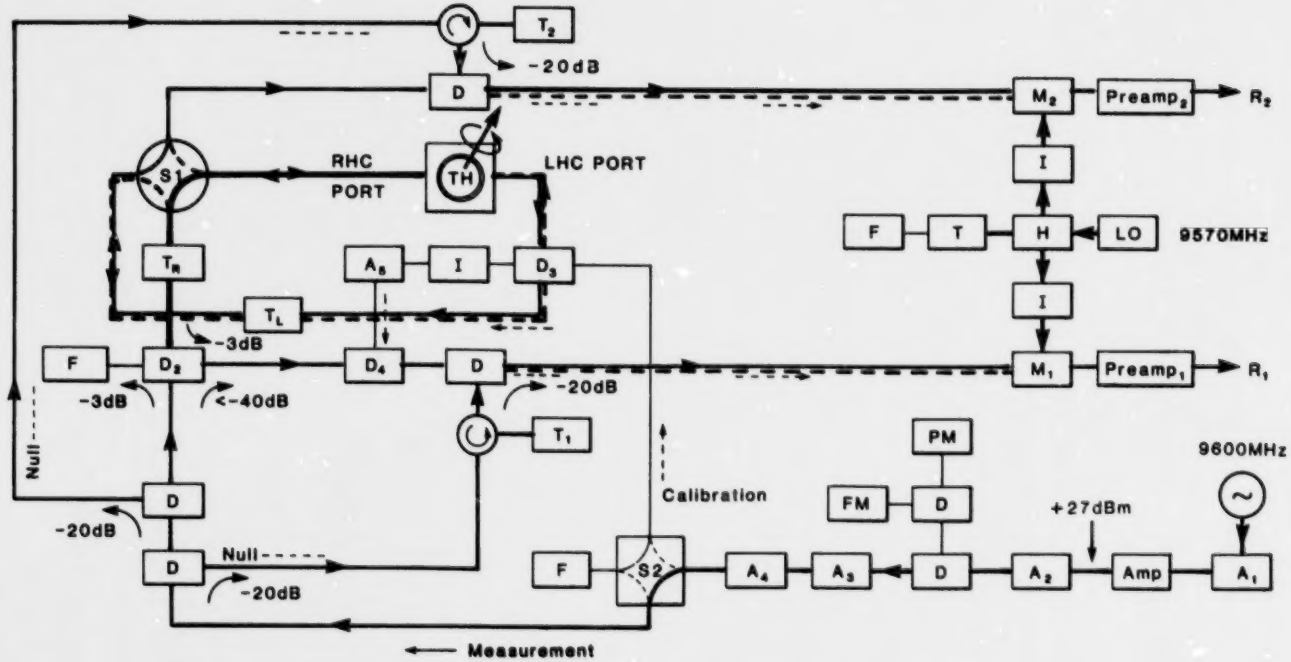

A_1	LEVEL SET ATTENUATOR (10dB)	FM	FREQUENCY METER
A_2	ATTENUATOR (0-20dB)	H	3dB HYBRID JUNCTION
A_3, A_4, A_5	ROTARY VANE ATTENUATOR (0-50dB)	I	ISOLATOR
Amp	POWER AMPLIFIER	LO	LOCAL OSCILLATOR
$PREAMP_1$, $PREAMP_2$	PREAMPLIFIER FOR RECEIVERS 1,2	M_1, M_2	MIXERS
C	CIRCULATOR	PM	POWER METER
D	20dB DIRECTIONAL COUPLER	S_1, S_2	WAVEGUIDE SWITCHES
D_2	3dB DIRECTIONAL COUPLER	T, T_R, T_L	TUNER
D_3	41dB DIRECTIONAL COUPLER	T_1, T_2	AMPLITUDE AND PHASE TUNER
D_4	29dB DIRECTIONAL COUPLER	TH	TURNSTILE - HORN
F	FLAT LOAD		

TRANS. SIGNAL
TARGET ECHOES
NULLING SIGNALS
LOCAL OSC

Figure 6. Complete block diagram of scattering system

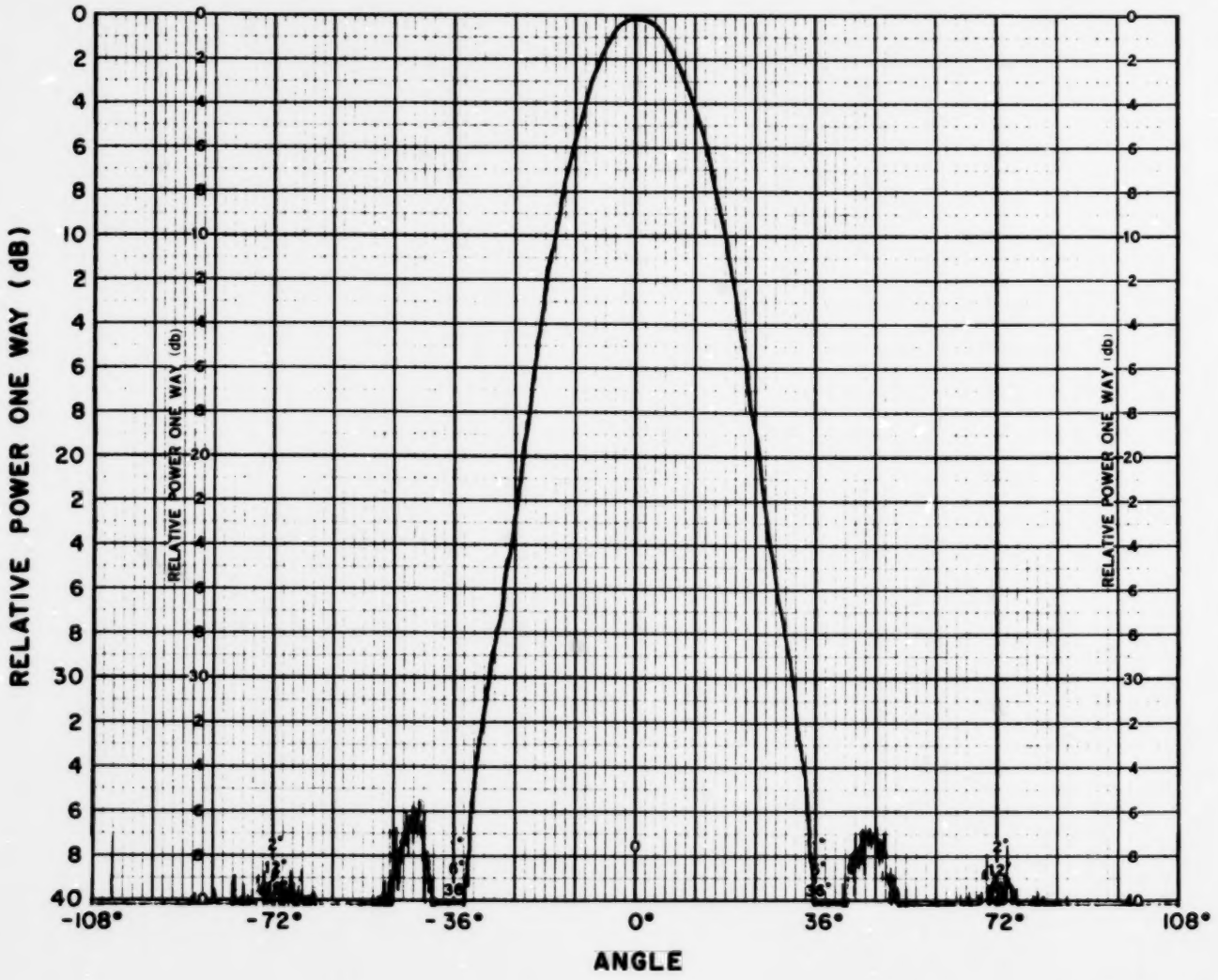

Figure 7. (a) X-band horn antenna amplitude pattern: Port 1, elevation plane

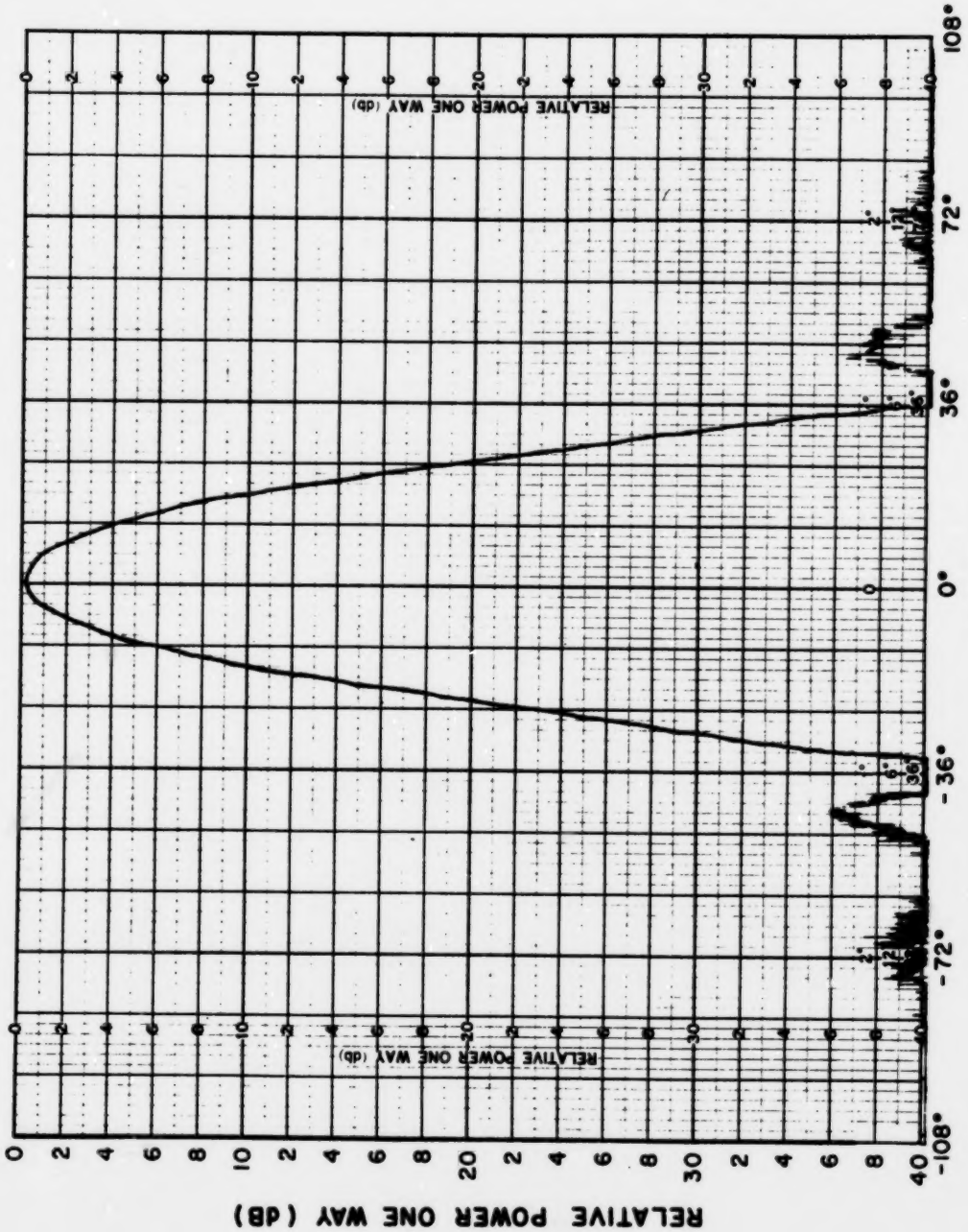

Figure 7. (b) X-band horn antenna amplitude pattern: Port 2, elevation plane

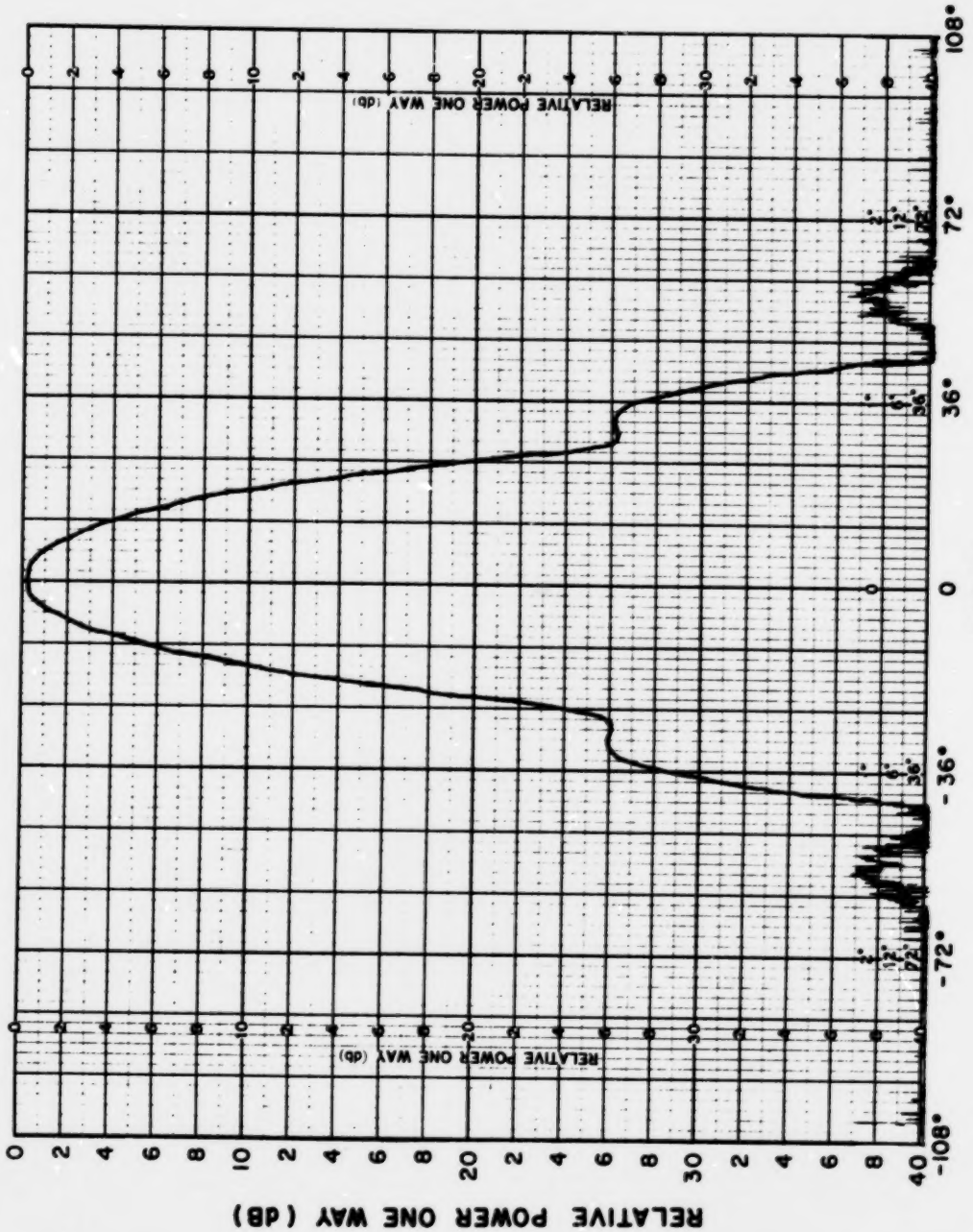

Figure 7. (c) X-band horn antenna amplitude pattern: Port 3, azimuth plane

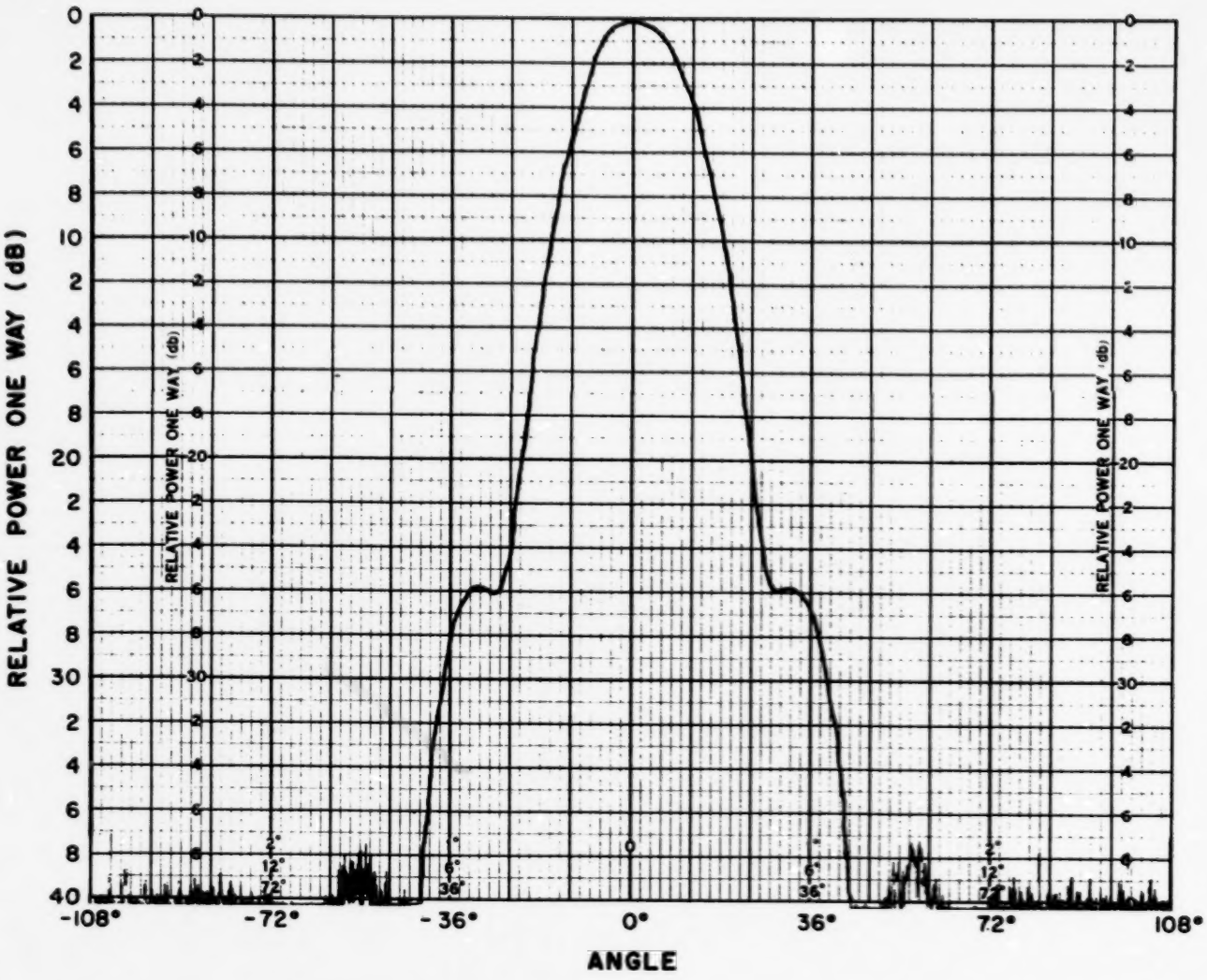

Figure 7. (d) X-band horn antenna amplitude pattern: Port 4, azimuth plane

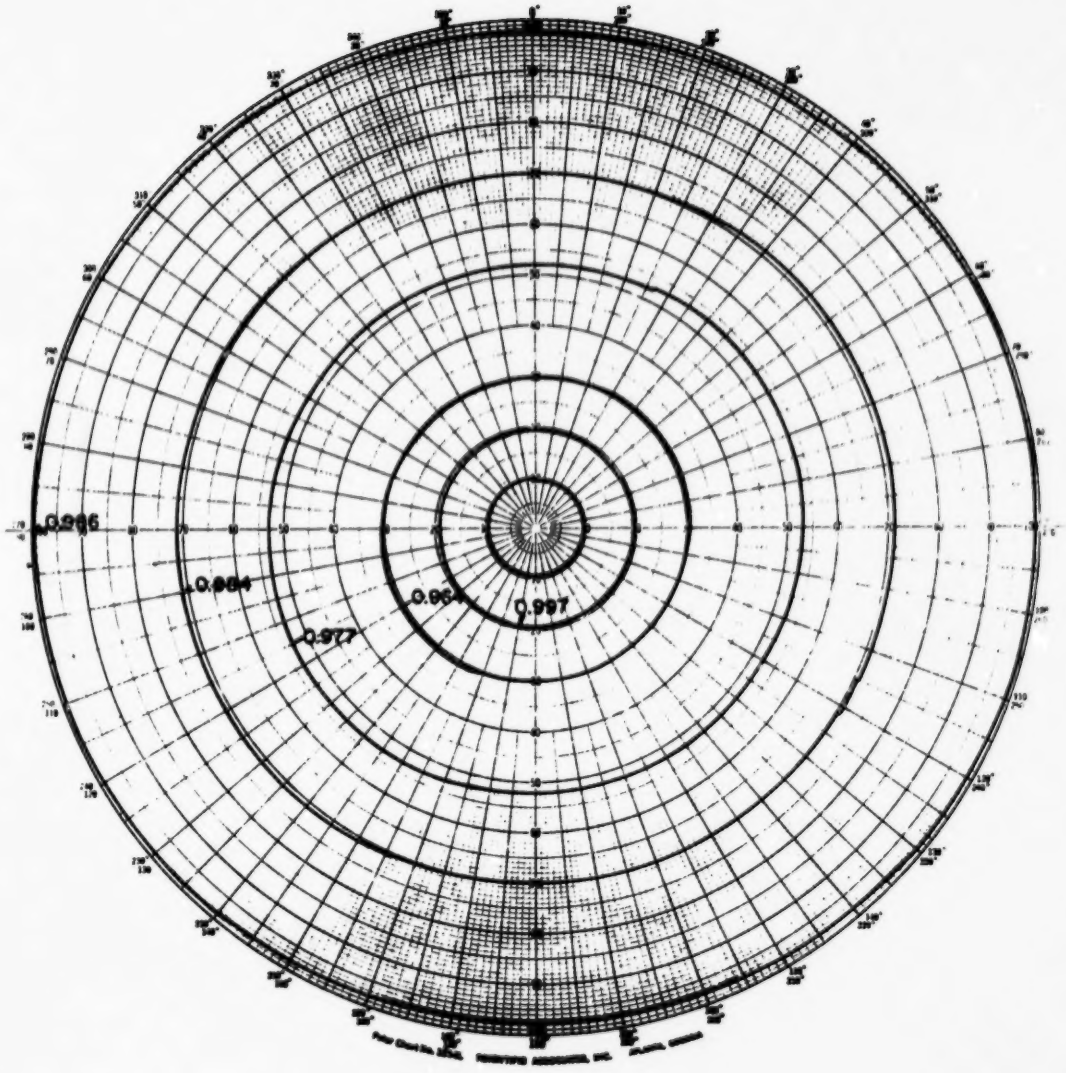

(a)

PORT 1

ELEVATION PLANE

Figure 8. X-band horn antenna polarization patterns, showing axial ratios at various points in the main beam

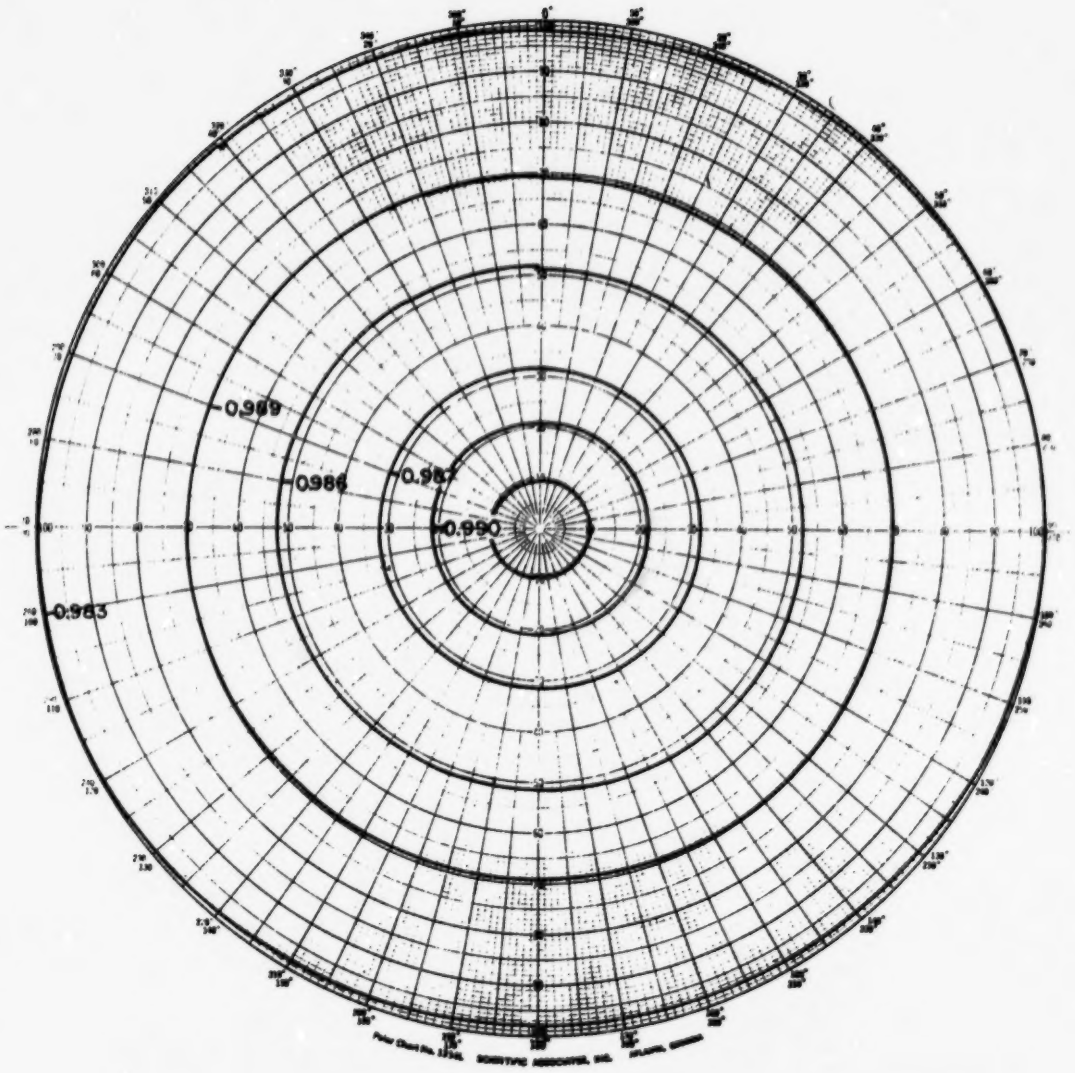

(b)

PORT 1

AZIMUTH PLANE

Figure 8 (Cont'd)

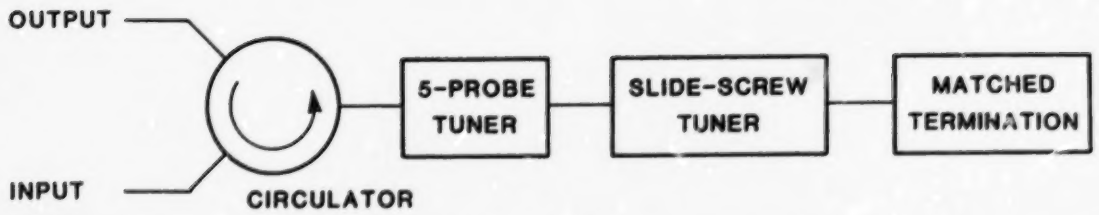

Figure 9. Amplitude and phase tuner assembly

directivity being in excess of 40 dB. Couplers D_3 and D_4 are crossguide devices with coupling factors of 41 and 29 dB, respectively. The decoupled signal in D_3 is used only in the calibration mode; in other operating modes both arms of D_3 function strictly as transmission paths.

4. ISOLATION, MATCHING, AND LEAKAGE SUPPRESSION MEASURES

The prevention of unwanted leakage and reflection of signals is of paramount interest, especially in a c-w system. Some of the measures taken to reduce these effects are described in this section.

A potentially serious leakage path is the local oscillator (LO) circuit. It is not uncommon for signal R_2 to exceed R_1 by 30 dB or more, in which circumstances even a small amount of leakage of the large signal can seriously contaminate the weaker signal. Fortunately it is relatively easy to reduce cross-coupling via the LO circuit to negligible levels. The mixers provide some isolation (of the order of 28 dB at X-band), and 20 dB or more is provided by the one isolator through which the leakage signal passes in the reverse direction. The hybrid junction will provide some isolation depending upon the VSWR of the oscillator. With use of a five-probe tuner and flat load on the unused port of the hybrid, the overall isolation of the LO circuit can be adjusted to a stable value of 70 dB, at which level leakage is negligible under all circumstances.

The turnstile junction is a critical component in two respects, namely, isolation and impedance matching. It must have high isolation between RHC and LHC ports, because excessive leakage caused by poor isolation is difficult to null out. Likewise a poorly matched device will reflect unmanagable amounts of power. The turnstile has been matched to a VSWR of less than 1.02 at each rectangular waveguide port, and the isolation between these is in excess of 45 dB. Figure 10 shows the isolation as a function of frequency.

Coupler D_2 must have high directivity so that the amount of the transmitted power coupled into Receiver No. 1 is managable. (The main function of D_2 is to segregate the transmitted and received signals of the same

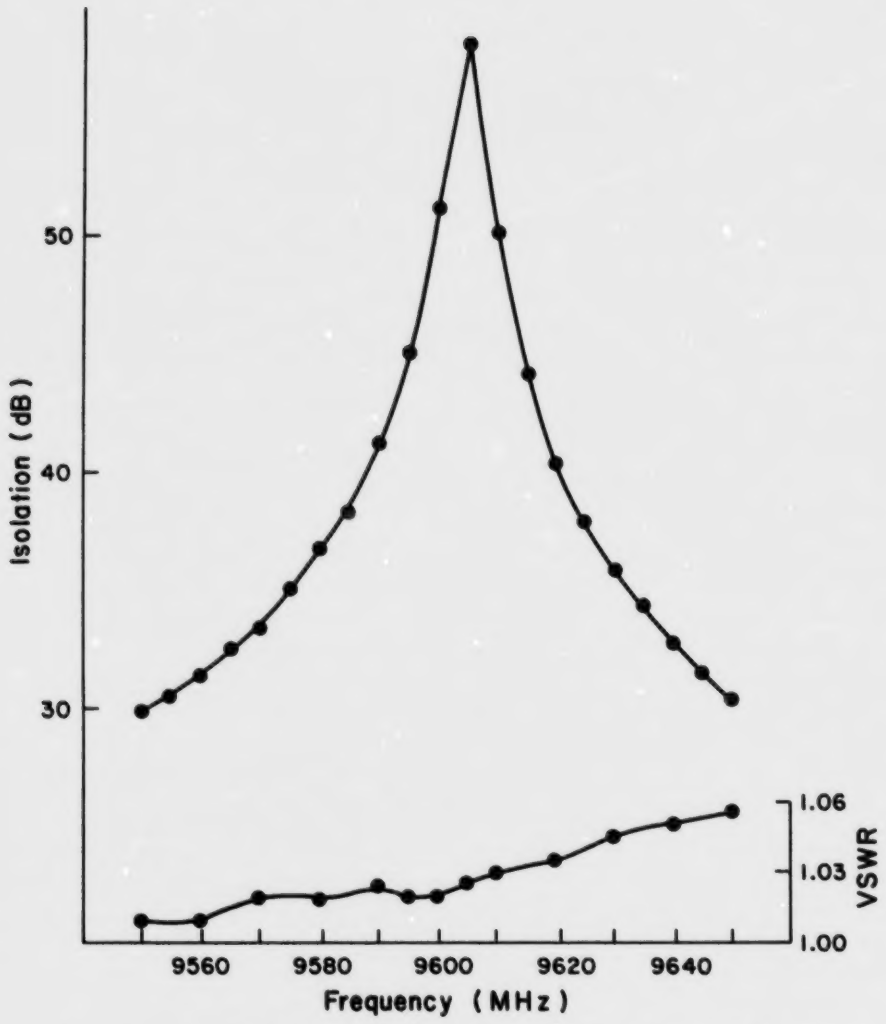

Figure 10. Isolation and VSWR of turnstile and horn

polarization. A high performance circulator could provide this duplexing function, but the directional coupler is more stable.)

Switch S_1 also has stringent specifications because transmitted and received signals coexist in this device. Ideally it should provide high and stable isolation with good repeatability when the switch is cycled. Leakage from the five-probe tuners is minimized by using dielectric extension rods on the tuning probes and enclosing these in beyond-cutoff cylindrical tubes. Finally, the joints between waveguide sections are all of the choke-to-flange type and are sealed with conducting paint where necessary.

5. NULLING PROCEDURE

Nulling of the system refers to cancelling the unwanted signals which remain at the receiver outputs in the absence of any echoing object within the field of view of the antenna. At best, nulls in the receiver outputs can only be achieved over a narrow frequency band and, because of thermal effects, can only be held for time periods of the order of two to three minutes. These intervals, however, are more than adequate for the completion of the measurement of a single object. Nulling is done before each measurement and is checked immediately after completion. Data are rejected if evidence of insufficient nulling is found in the post-observation check.

The method of nulling may be explained with reference to Fig. 11. First, with RHC polarization chosen, tuner T_R is adjusted to reduce the reflections from the turnstile and horn to a level of -40 dB or lower. This puts the unwanted signal into a range where it can be further nulled by tuner T_1. Adjustment of the latter then follows, to reduce the residual signal to less than noise level at the output of Receiver No. 1. Similarly, T_2 is adjusted to reduce the residual output of Receiver No. 2. Second, with LHC polarization chosen by S_1, tuner T_L is adjusted to reduce the composite reflections at D_2 to below -40 dB, following which T_1 and T_2 can be used to null the residual signal outputs of Receivers 1 and 2, respectively. When the polarization is changed via S_1, it is necessary to readjust $T_1$and T_2, but $T_R$and T_L do not have to be readjusted.

6. RECEIVING SYSTEM

As described earlier, the scattering matrix apparatus utilizes a large portion of the precipitation radar receiving system for reasons of economy. The output of the scattering measurement facility comprises two 30 MHz signals, which are transmitted to the radar equipment room via coaxial cables. These two signals are then fed into the radar receiving system in lieu of the corresponding radar signals. The radar receiving system provides for the measurement of the amplitudes of the two orthogonal signals, their relative electrical phase, and the degree of cross-correlation between them. (Because all the signals are continuous wave in the scattering experiment and only a single particle is being illuminated, there is always 100% cross-correlation, and thus the cross-correlation part of the measurement capability is not needed.)

The basic elements of the receiving system are shown in the block diagram of Fig. 12. (The integrators and range gates shown in ref. 4 are not used because of the c-w nature of the signals.) The dynamic range of

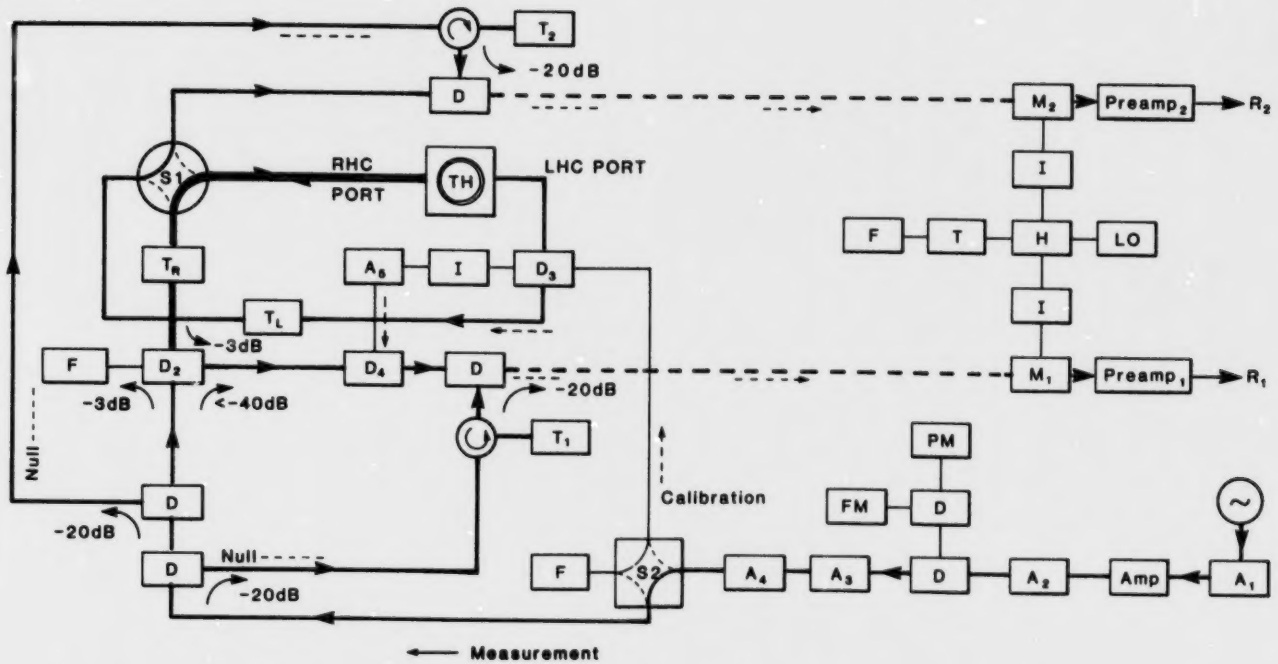

A_1	LEVEL SET ATTENUATOR (10dB)	FM	FREQUENCY METER
A_2	ATTENUATOR (0-20dB)	H	3dB HYBRID JUNCTION
A_3, A_4, A_5	ROTARY VANE ATTENUATOR (0-50dB)	I	ISOLATOR
Amp	POWER AMPLIFIER	LO	LOCAL OSCILLATOR
$PREAMP_1$, $PREAMP_2$	PREAMPLIFIER FOR RECEIVERS 1,2	M_1, M_2	MIXERS
C	CIRCULATOR	PM	POWER METER
D	20dB DIRECTIONAL COUPLER	S_1, S_2	WAVEGUIDE SWITCHES
D_2	3dB DIRECTIONAL COUPLER	T, T_R, T_L	TUNER
D_3	41dB DIRECTIONAL COUPLER	T_1, T_2	AMPLITUDE AND PHASE TUNER
D_4	29dB DIRECTIONAL COUPLER	TH	TURNSTILE - HORN
F	FLAT LOAD		

TRANS. PWR →

REFLECTIONS & LEAKAGE →

NULLING SIGNALS →

Figure 11. Nulling procedure

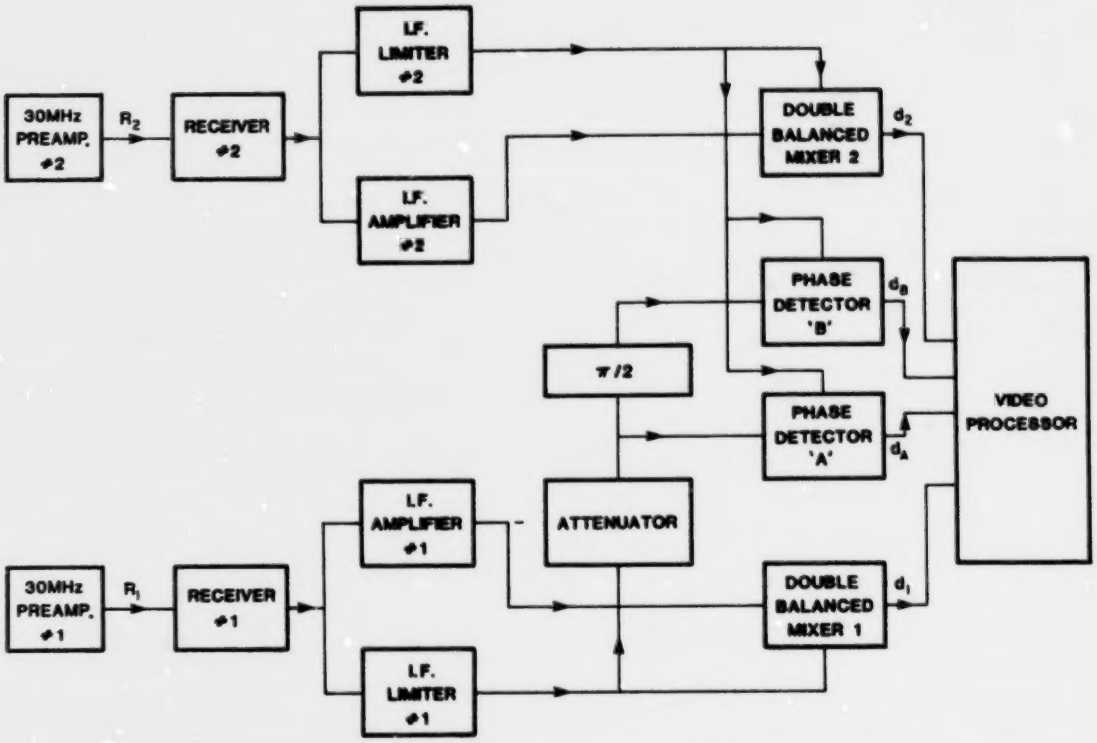

Figure 12. Receiving system

the system, at any particular setting of the attenuators, is approximately 35 dB, with Receiver No. 1 being the limiting element. Receiver No. 2 has a dynamic range of about 40 dB. These operating ranges may be extended by appropriate adjustment of the attenuators. For example, to probe a deep null, the radiated power level may be increased temporarily during part of the recording process, and the results so obtained matched up with other results taken with normal power levels at angular settings away from the null.

The amplitude linearity is shown by the receiver transfer characteristics of Fig. 13. It may be seen that Receiver 2 has a greater linear range than does Receiver 1. Deviations from constant phase angle are shown in Fig. 14, which is a phase error matrix for joint variations in the signal levels of the two receivers. Phase errors were minimized in the design of the receiver system by minimizing phase variations vs. amplitude level for each receiver individually, and then equalizing the phase/frequency slopes (i.e., $\Delta\phi/\Delta f$) for the i-f chains by inserting a coaxial cable loop in one receiver of length such that, with a common input, the differential phase between receiver outputs was approximately constant over the

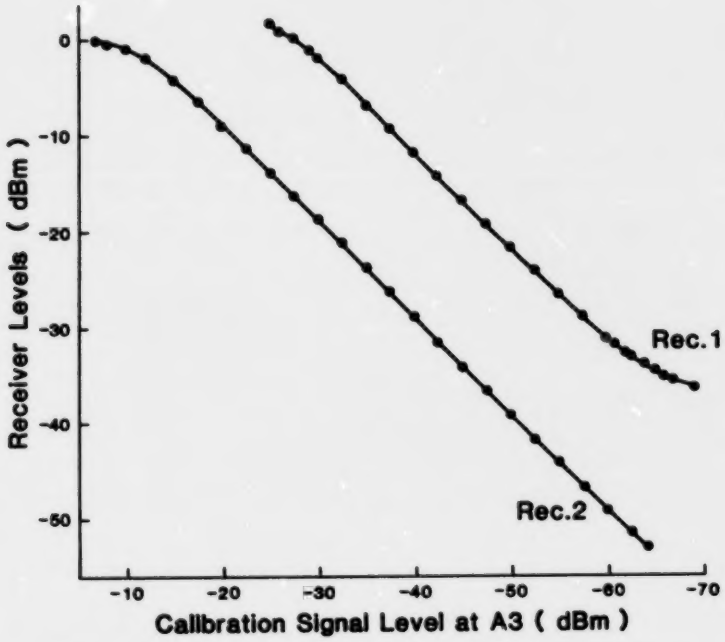

Figure 13. Receiver transfer characteristics

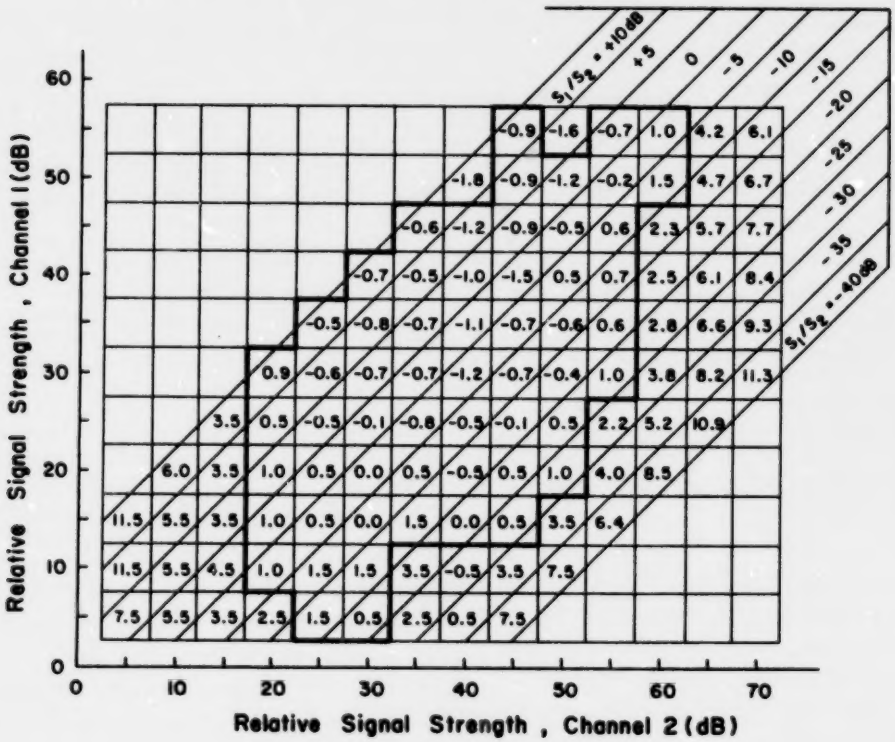

Figure 14. Phase error matrix

receiver bandpass. (It should be noted that this requirement is much more important for radar signals, which encompass a significant bandwidth, than it is for the scattering experiment signals, which are nearly monochromatic.)

The receiving system output comprises four analog voltages, which are proportional, respectively, to $(R_1R_1^*)^{1/2}$, $(R_2R_2^*)^{1/2}$, cos (arg $R_1R_2^*$), and sin (arg $R_1R_2^*$) (subject to fixed phase shifts which are embedded in the overall calibration). Thus the power levels in each channel and the in-phase and quadrature components of the cross-product are available. The relative phase of the returns is directly obtainable from the cross-product components.

7. DATA ACQUISITION SYSTEM

As in the case of the receiving system, use is made of the precipitation radar data acquisition apparatus for the scattering matrix measurements. Figure 15 shows the main element in block diagram form. Data acquisition is controlled by a system clock/controller at a 10-Hz rate. Under control of the clock, the four analog outputs of the receiving system are scanned and digitized sequentially, at a scan rate of 10 per second, by the A/D converter. Also digitized in each scan is a voltage adjustable in increments of 0.1 V for coding purposes, and an internal reference signal which serves as a zero in the A/D converter. The outputs of the A/D

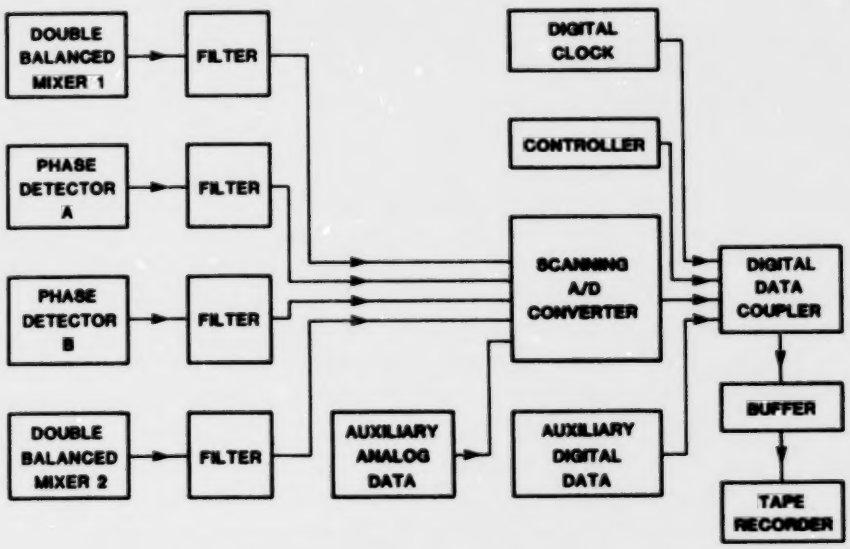

Figure 15. Video processor and data recording system

converter are combined in the Data Coupler with the time (from a digital clock) and with record header data which serves to identify and code the data record. The combined data are then transferred from the coupler to a buffer memory and then to a nine-track magnetic tape, which is processed at the NRCC Computation Centre after completion of the measurements.

The sample under test is rotated uniformly at a rate of approximately 3-1/3 rpm (20°/s). At a scan rate of 10 per second, individual readings are therefore obtained at increments of about 2.0°. Sixteen scans comprise one record, so that a complete 360° rotation requires just over 11 records at that scan rate. Faster scan rates are available if required.

8. CALIBRATION

System calibration involves four separate quantities. These are: (a) the variations in phase with changes in operating levels; (b) the departure of the input-output amplitude characteristics from a linear relationship; (c) for those measurements made within the near field, the range dependence of the output amplitude from a known target as it is moved radially within the field of the illuminating antenna; and (d) the relationship of the output amplitudes to the expected backscattering amplitudes from known targets, e.g., small metal spheres. The latter is an absolute calibration.

In addition, the system is checked with short metal rods, which, as targets, produce equal amplitude echoes in the two channels. The lateral uniformity of the illuminated echoing region is determined with a metal sphere. The latter check determines the useful echoing area within which the target may be placed.

Phase and amplitude calibrations are performed at the beginning or end of each day of observations. The method of phase calibration is illustrated in Fig. 16. With switch S_2 set to the calibration position, directional couplers D_3 and D_4 inject signals from the source oscillator into Receivers 2 and 1, respectively. Attenuators A_3 and A_5 are then adjusted to provide a variety of absolute and relative levels in the waveguides leading to the two receivers. (If required, attenuator A_4 may also be used to extend the range of variation of the signal in Receiver No. 1.) Specifically, at a given setting of A_3, the setting of A_5 is varied in 5-dB steps. At each step, the relative phase of R_1 and R_2 is determined. A_3 is then adjusted by 5 dB, and A_5 is again stepped through its range. The process is repeated until a two-dimensional array of relative phases is generated. This array presents input to one stage of the computation where further processing of the error values to get a finer array is done. In particular,

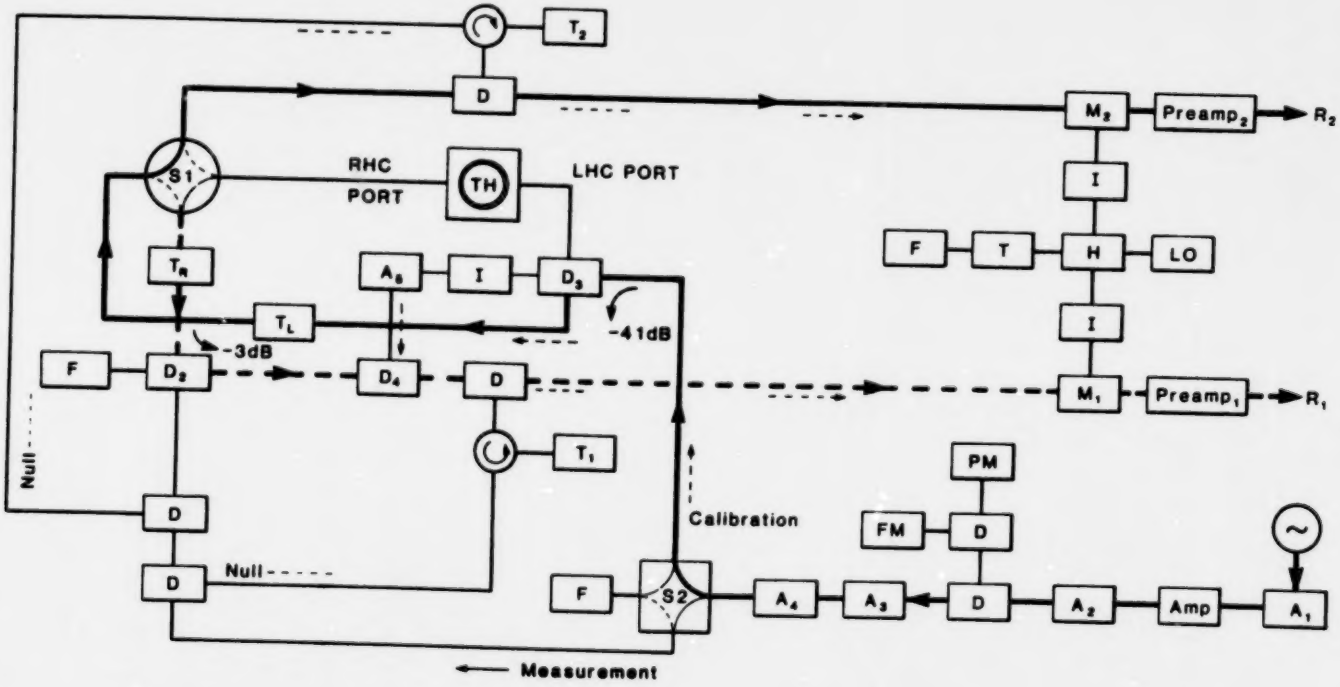

A_1	LEVEL SET ATTENUATOR (10dB)
A_2	ATTENUATOR (0-20dB)
A_3, A_4, A_5	ROTARY VANE ATTENUATOR (0-50dB)
Amp	POWER AMPLIFIER
$PREAMP_1$, $PREAMP_2$	PREAMPLIFIER FOR RECEIVERS 1,2
C	CIRCULATOR
D	20dB DIRECTIONAL COUPLER
D_2	3dB DIRECTIONAL COUPLER
D_3	41dB DIRECTIONAL COUPLER
D_4	29dB DIRECTIONAL COUPLER
F	FLAT LOAD
FM	FREQUENCY METER
H	3dB HYBRID JUNCTION
I	ISOLATOR
LO	LOCAL OSCILLATOR
M_1, M_2	MIXERS
PM	POWER METER
S_1, S_2	WAVEGUIDE SWITCHES
T, T_R, T_L	TUNER
T_1, T_2	AMPLITUDE AND PHASE TUNER
TH	TURNSTILE - HORN

Figure 16. Phase calibration procedure

using some available software a smoother array of the relative phase values, for variation of 1 dB in the levels of the channels, is generated. This latter array is used in the final calculations of the data on the samples.

Amplitude calibration (Fig. 17) is performed in a similar fashion, although the linearity of the receivers is determined sequentially, with S_1 set to deliver the calibration signal to Receiver 1 or Receiver 2 as desired. The input signal amplitude is varied by Attenuator A_3 to generate transfer curves for the receivers. (This information can also be retrieved from the phase calibration.) To account for any nonlinearity in the data a cubic spline interpolation procedure is used to generate a best fit to the data. The spline coefficients are then used to set up a table of voltages vs. decibel values for each channel. These tables are used in the final computation on the data.

The range dependence in the operating region of the antenna is given by the function K(R), which, for the far-field region would simply be R^{-4}. An example of empirical determinations of K(R) for two different metallic sphere diameters is shown in Fig. 18.

9. PERFORMANCE AND TECHNICAL SPECIFICATIONS

This section describes some of the performance characteristics of the equipment which have not been dealt with elsewhere in the report. The main technical characteristics pertain to sensitivity, leakage (which governs the achievable null depth), dynamic range, and usable echoing area. Also important are the data rate and the rotational rate for the samples.

Because the minimum usable signal level is determined primarily by leakage and the stability of the nulling procedure, no particular attempt has been made to achieve high sensitivity. The mixer-preamplifier combinations used have a noise figure of approximately 9 dB and have a bandwidth of about 4 MHz. Thus for unity signal-to-noise ratio, the receiver input signal level is FkT_oB, i.e., -99 dBm, a value which could, if necessary, be reduced substantially by decreasing the i-f bandwidth, since the received signal is nearly monochromatic. In practice, such a reduction is not particularly rewarding, because, as pointed out above, the measurements are rarely noise limited.

The depth of null which can be achieved is sufficient to reduce the leakage to noise level (or below) for periods of 2 to 3 min at a time before re-nulling becomes necessary. Since a complete 360° rotation of the sample is accomplished in 18 s, data over several complete rotations of the object will be obtained before re-nulling is required.

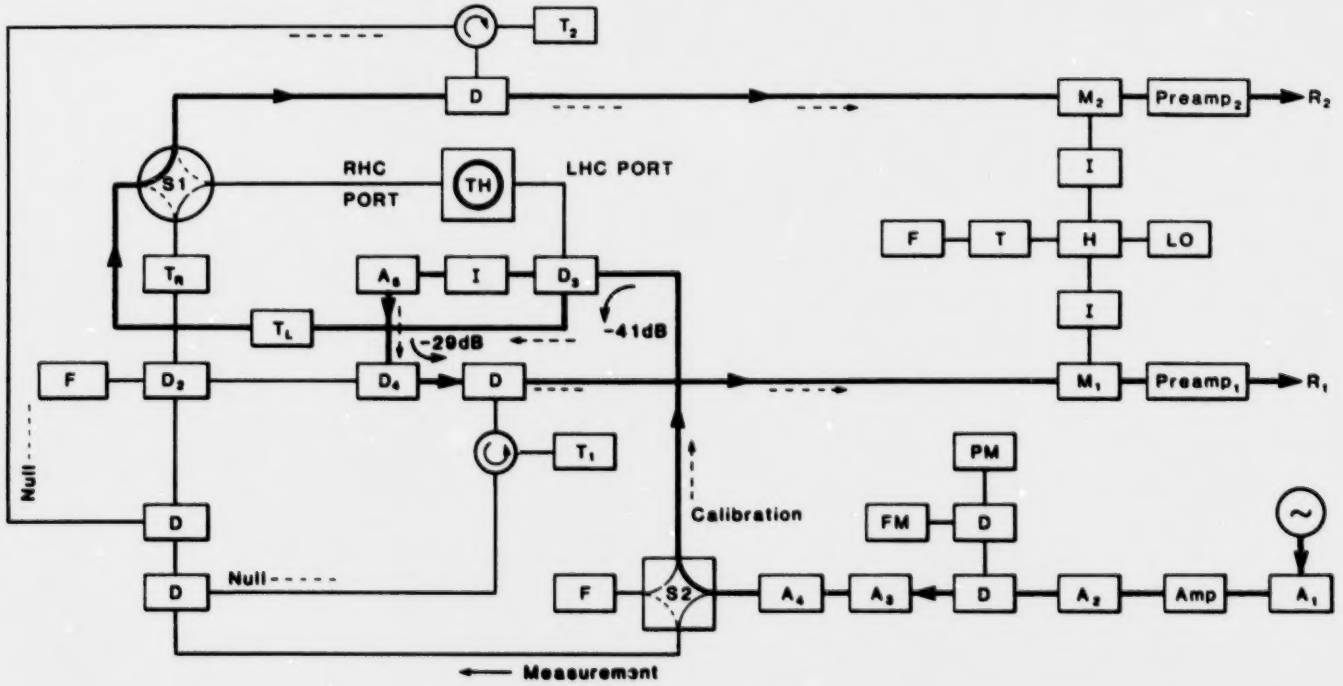

A_1	LEVEL SET ATTENUATOR (10dB)	FM	FREQUENCY METER
A_2	ATTENUATOR (0-20dB)	H	3dB HYBRID JUNCTION
A_3, A_4, A_6	ROTARY VANE ATTENUATOR (0-50dB)	I	ISOLATOR
Amp	POWER AMPLIFIER	LO	LOCAL OSCILLATOR
$PREAMP_1$, $PREAMP_2$	PREAMPLIFIER FOR RECEIVERS 1,2	M_1, M_2	MIXERS
C	CIRCULATOR	PM	POWER METER
D	20dB DIRECTIONAL COUPLER	S_1, S_2	WAVEGUIDE SWITCHES
D_2	3dB DIRECTIONAL COUPLER	T, T_R, T_L	TUNER
D_3	41dB DIRECTIONAL COUPLER	T_1, T_2	AMPLITUDE AND PHASE TUNER
D_4	29dB DIRECTIONAL COUPLER	TH	TURNSTILE - HORN
F	FLAT LOAD		

Figure 17. Amplitude calibration procedure

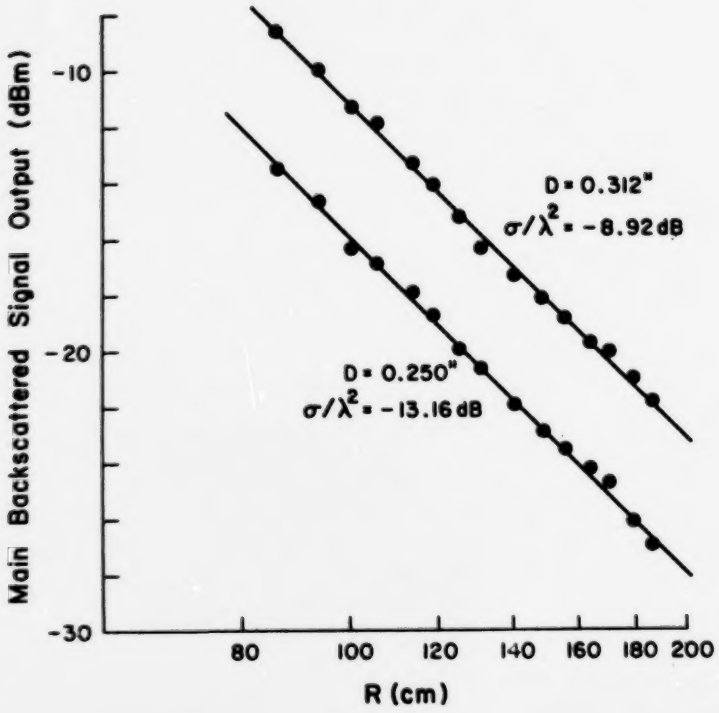

Figure 18: Determination of K(R) for X-band system. Solid lines slope at -12 dB per octave, corresponding to R^{-4} signal level dependence

The usable echoing area is determined by the antenna beamwidth characteristics and by the maximum distance from the horn at which the object can be situated and still provide echoes of sufficient strength. For the larger objects, which are usually placed about 180 cm from the horn, the usable echoing area is circular with a diameter of the order of 20 cm. For smaller objects, which have to be positioned at 75 to 100 cm above the horn, the usable area is proportionately smaller. In each case the determining factor is the constancy of amplitude and phase of the illuminating wave over the illuminated area.

For a radiated power level of +22 dBm at X-band, the cross-sectional echoing area σ, for unity signal-to-noise ratio in the main receiving channel with an object at a height of 100 cm from the horn, is 1.02×10^{-10} m^2. Usually, however, all the scattering matrix elements of an object this small would not be measurable since the echo of the opposite sense tends to be much weaker than that in the main channel, especially for small objects. For example, if the cancellation ($10 \log |\nu|^2$) is say -30 dB, then the minimum cross-sectional area for which σ and ν are measurable would be at

least 10^{-7} m^2 at that height. In practice, if the angle δ is to be measured accurately, an increase in σ, to provide echoes clearly above the noise level, is required.

10. EXPERIMENTAL PROCEDURE

To conduct measurements, the object whose scattering matrix is to be determined is suspended above the vertically-pointing horn antenna by a pair of nylon threads, 0.008 to 0.012 in. diameter, which pass through small holes drilled near the edges of the object. These threads are stretched tightly between supports which are outside of the illuminated area. Two threads are used so as to permit rotation of the object about an axis parallel to the mounting threads. On one of the supports, the threads are attached to a motor-driven rotator.

For small objects, the rotation rate of the object is uniform, but larger samples, particularly those of high eccentricity, tend to rotate non-uniformly because of the varying effects of gravitational forces on the suspension system. If necessary, video recording of the object and a digital time display could be used to assist in determining the rotational position of the object.

Normally, RHC and LHC recordings, which are done separately, are combined. If desired, however, the RHC and LHC data may be separately plotted. Such separation would be indicated if, for example, it is suspected that the object being measured exhibits some helicity or other RHC-LHC inequality.

All controls for the experiment are in the scattering equipment shack, including those for the data acquisition equipment, which is situated some distance away in the radar equipment room. Voltages proportional to the amplitudes of the signals in each channel are fed back to the equipment site and are displayed for the operator to monitor during observations. This ensures that the signal levels can be maintained at an appropriate level.

The local oscillator frequency is not automatically controlled, however its frequency is continuously displayed for the operator, who may adjust it if necessary by means of voltage tuning. Such tuning is needed only infrequently because this frequency is highly stable.

For identification purposes, a coding voltage (one of 100 distinct levels) is recorded before the start and at the end of the observations for each sample. When the sample is in the field for recording data this voltage conveys information on the rotation angle of the sample.

Data may be taken either under static (non-rotating) or dynamic (rotating) conditions. The data sampling interval may be varied as appropriate, with intervals of 0.025 to 0.1 s being commonly used.

11. DATA RECORDING FORMAT AND INTERPRETATION

Raw data are recorded on nine-track tape at 800 BPI using BCD code. Thus only five tracks are used, including the parity bit track. Bit weights 1-2-4-8 are assigned to tracks 2-8-1-9, respectively, while the parity bit is on track 4. The word format is established by the Data Coupler. Each word consists of six characters of four bits each, with successive words recorded contiguously on the tape. The record length, also established by the Coupler, is 678 characters (i.e., 113 words). A complete record requires 16 consecutive scans through the input channels. The first scan generates eight words (header, clock, internal reference channel, four data words, and a code word, in that order). The 15 succeeding scans comprise seven words each, since the header word is recorded only once per record. An inter-record gap is generated by the Coupler and is automatically inserted after each 113 words.

Typically, about 4000 records, comprising measurements on samples or calibration, are accumulated on a tape before being sent to the Computer Centre for analysis. The first step in the computation is to interpret the data and generate a printout of all records on the tape to examine the quality of the data. During this process initial calculation are performed to obtain a rough estimate of the phase between R_1 and R_2, the ratio v^2, and the main return $(R_2\ R_2^*)^{1/2}$. The next step in the computation is to edit the data, disregard the useless records, and back up the good data on Computer Centre tapes for the final accurate calculations. The latter incorporates corrections for phase error and amplitude nonlinearity of the system, performs normalization, and corrects for errors as explained in the next section.

12. ERROR CORRECTION AND NORMALIZATION

In addition to the phase and amplitude calibration data and range dependence function K(R) discussed in Section 8, further constants are required for the final analysis of the data. These include the absolute level normalization for the main backscatter return $(R_2\ R_2^*)^{1/2}$, adjustments needed to normalize the relative amplitudes and phases in the two receivers, for each switch position, and the polarization error term $\varepsilon_{\pm}$.

The voltage corresponding to $(R_2\ R_2^*)^{1/2}$ is normalized against backscatter data of small metallic spheres, for which tables of radar cross-

section are available (5). A dipole of length 0.3λ is used as a target, for normalization of the relative amplitudes and phases in the receivers. For either RHC or LHC transmission, the received components from the dipole should have equal amplitudes and phase. Thus, any differential gain in the receivers can be determined, and a phase reference is set for each switch position. The complex error term $\varepsilon_{\pm}$ in Equation [11] is determined from data taken on small spheres, for which ideally η should be zero.

The normalization constants, complex error term, phase and amplitude calibration tables are all provided for the final stage of calculation and plotting of the data. Further details on the programs and computation are available from the authors.

13. SAMPLE OF RESULTS

Extensive results with this apparatus have been reported (6-8). A sample of the results is included here for illustrative purposes.

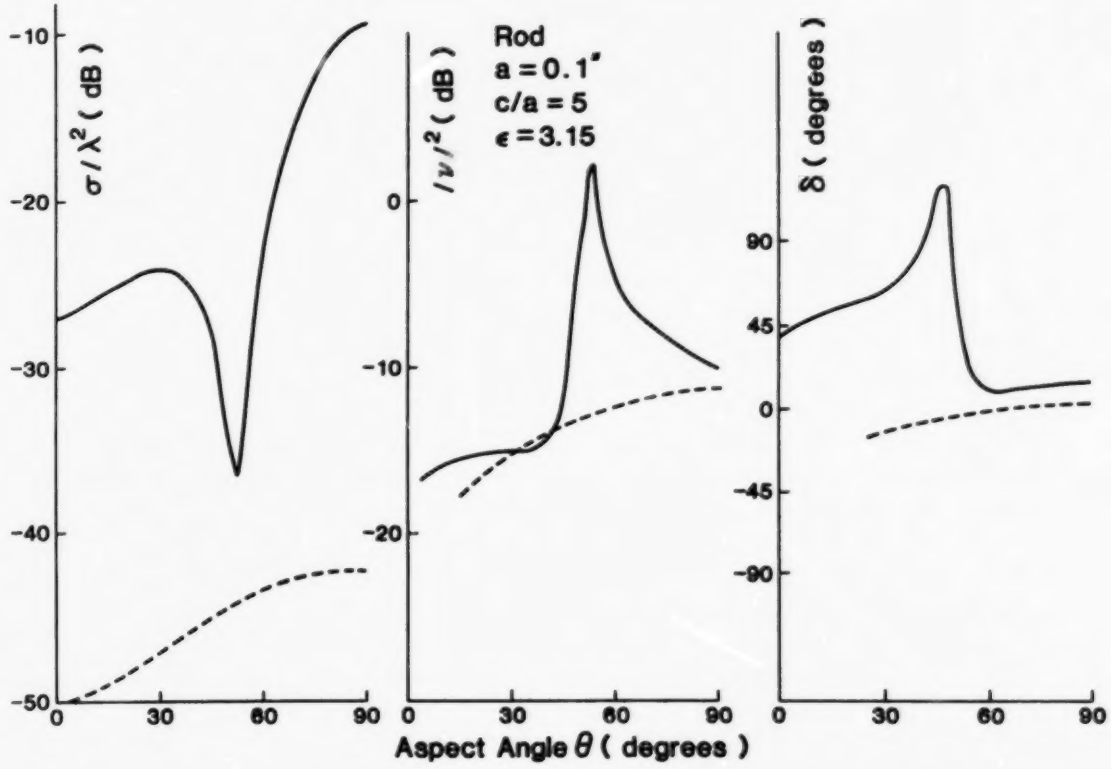

Scattering coefficients for one sample at 2.862 GHz ---, and at 9.6 GHz ——.

Figure 19. Sample of results for a dielectric rod.
ka = 0.152 at 2.862 GHz, 0.511 at 9.6 GHz.

Figure 19 shows three parameters for a rod of length 1 in., diameter, 0.2 in., having a relative dielectric constant of 3.15. The values are shown for two frequencies, namely 2.862 GHz (dashed curves) and 9.600 GHz (solid curves). The left-hand panel shows the backscattering cross-section, σ, normalized in terms of square wavelengths, as a function of aspect angle. The magnitude $|\nu|^2$ and δ, the backscattering differential phase shift for circular polarization, are shown in the remaining two panels. At the lower frequency, this object has a ka value (where $k = 2\pi/\lambda$) of 0.152, λ being the free space wavelength, while at the higher frequency, ka = 0.510. The smooth curves at 2.862 GHz are characteristic of scattering objects well below the resonance region, while the effect of resonances is strikingly evident in the 9.600 GHz data. Note that at an aspect angle near 53°, the same-sense echo exceeds that of the opposite sense echo, as shown by the positive values of $|\nu|^2$ in that region. A sharp variation in δ and a deep notch in the σ value also characterize backscattering at this aspect. Results for rods of other sizes, as well as for disks, and oblate and prolate spheroids, may be seen in the published data referred to above.

ACKNOWLEDGEMENT

The authors wish to acknowledge the many contributions of Dr. G.C. McCormick to the planning, development, and commissioning of the equipment described in this report. These contributions extended from the initial concepts through to the successful operation of the facility.

REFERENCES

1. G.C. McCormick and A. Hendry. Principles for the radar determination of the polarization properties of precipitation. Radio Sci., 10: 421-434; 1975.

2. P.D. Potter. A new horn antenna with suppressed sidelobes and equal beamwidths. Microwave J. 6: 71-78, 1963.

3. G.L. Ragan, Microwave Transmission Circuits Radiation Laboratory Series 1948. Vol. 9, p. 375.

4. G.C. McCormick and A. Hendry. Techniques for the determination of the polarization properties of precipitation. Radio Sci. 14: 1027-1040; 1979.

5. J.W. Crispin, Jr., and K.M. Siegel (Editors). Methods of Radar Cross-section Analysis. Academic Press, New York. 1968.

6. L.E. Allan and G.C. McCormick. Measurements of the backscatter matrix of dielectric spheroids. IEEE Trans. Antennas Propag. AP-26: 579-587, 1978.

7. L.E. Allan and G.C. McCormick. Measurements of the backscatter matrix of dielectric bodies. IEEE Trans. Antennas Propag. AP-28: 166-169; 1980.

8. L.E. Allan and G.C. McCormick. Measurements of the backscatter matrix of dielectric bodies. NRC/ERB-921, Division of Electrical Engineering, National Research Council of Canada, Ottawa, Ont. March 1980.